



HHS Public Access

Author manuscript

Anal Chem. Author manuscript; available in PMC 2017 October 04.

Published in final edited form as:

Anal Chem. 2017 April 18; 89(8): 4628–4634. doi:10.1021/acs.analchem.7b00185.

Serpentine Ultralong Path with Extended Routing (SUPER) High Resolution Traveling Wave Ion Mobility-MS using Structures for Lossless Ion Manipulations

Liulin Deng[#], Ian K. Webb[#], Sandilya V. B. Garimella, Ahmed M. Hamid, Xueyun Zheng, Randolph V. Norheim, Spencer A. Prost, Gordon A. Anderson, Jeremy A. Sandoval, Erin S. Baker, Yehia M. Ibrahim, and Richard D. Smith^{*}

Biological Sciences Division, Environmental Molecular Sciences Laboratory, Pacific Northwest National Laboratory, 902 Battelle Boulevard, P.O. Box 999, MSIN K8-98, Richland, Washington 99352, United States

Abstract

Ion mobility (IM) separations have a broad range of analytical applications, but insufficient resolution often limits their utility. Here, we report on ion mobility separations in a structures for lossless ion manipulations (SLIM) serpentine ultralong path with extended routing (SUPER) traveling wave (TW) ion mobility (IM) module in conjunction with mass spectrometry (MS). Ions were confined in the SLIM by rf fields in conjunction with a DC guard bias, enabling essentially lossless TW transmission over greatly extended paths. The extended routing utilized multiple passes (e.g., ~1094 m over 81 passes through the 13.5 m serpentine path) and was facilitated by the introduction of a lossless ion switch that allowed ions to be directed to either the MS detector or for another pass through the serpentine separation region, allowing theoretically unlimited IM path lengths. The multipass SUPER IM-MS provided resolution approximately proportional to the square root of the number of passes (or total path length). More than 30-fold higher IM resolution (~340 vs ~10) for Agilent tuning mix m/z 622 and 922 ions was achieved for 40 passes compared to commercially available drift tube IM and other TWIM-based platforms. An initial evaluation of the isomeric sugars lacto-*N*-hexaose and lacto-*N*-neohexaose showed the isomeric structures to be baseline resolved, and a new conformational feature for lacto-*N*-neohexaose was revealed after 9 passes. The new SLIM SUPER high resolution TWIM platform has broad utility in conjunction with MS and is expected to enable a broad range of previously challenging or intractable separations.

Graphical Abstract

^{*}Corresponding Author: Phone: 509-371-6576. Fax: 509-371-6564. rds@pnnl.gov.

[#]Author Contributions

L.D. and I.K.W. contributed equally.

ORCID

Xueyun Zheng: 0000-0001-9782-4521

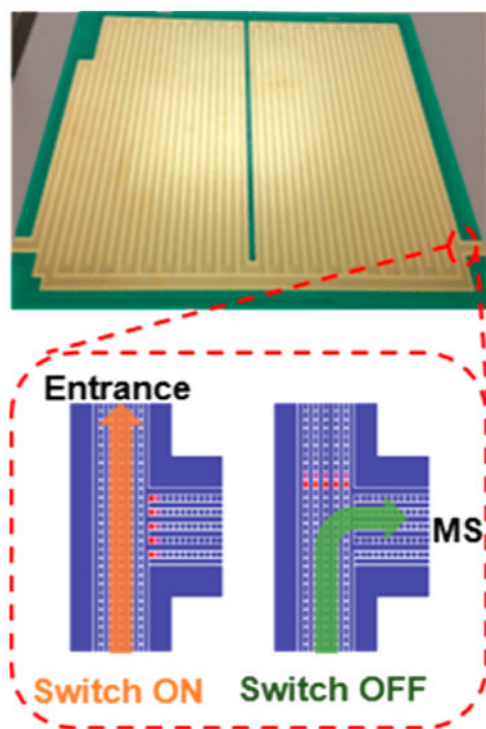
Erin S. Baker: 0000-0001-5246-2213

Yehia M. Ibrahim: 0000-0001-6085-193X

Richard D. Smith: 0000-0002-2381-2349

Notes

The authors declare no competing financial interest.



Ion mobility-mass spectrometry (IM-MS) is a powerful and versatile tool for both analytical applications and structural characterization.¹ IM separates ions in the gas-phase based upon size/shape-to-charge ratios. Higher-resolution IM approaches have shown utility for separating some conformations² and isomers,³ for biomolecule structural studies,⁴ and, increasingly, for analysis of “omics” mixtures.⁵ The recent wider adoption of IM-MS is attributed not only to the increasingly available commercial instrumentation, but also to its applicability across biomolecular classes (e.g., carbohydrates, lipids, peptides) and analysis speed. Indeed, IM separations achieving similar peak capacities as liquid chromatography (e.g., ~400 for peptides in a 90 min gradient)⁶ would potentially be transformative for many applications.

While several IM approaches have been reported that can achieve higher resolution separations, each has significant limitations. For example, field asymmetric waveform ion mobility spectrometry (FAIMS), using a planar electrode geometry,⁷ a mixture of helium or hydrogen with nitrogen as a carrier gas,⁸ increased field strengths,⁹ or reduced gas flow rate to provide greater separation times¹⁰ provides greatly increased resolution, but only in conjunction with large ion losses¹¹ as well as with lengthy scanning of the compensation voltage.¹²

Most higher resolution IM platforms separate ions in relatively weak (<20 V/cm) and uniform DC electric fields where mobility is not field dependent^{13,14} and where separation times vary linearly with mobility. Drift tube ion mobility (DTIM) generally analyzes ion pulses or packets, where the resolution (R) of two peaks is given by

$$R_{\text{DT}} = 2 \frac{t_2 - t_1}{\text{fwhm}_1 + \text{fwhm}_2} \quad (1)$$

where t_2 and t_1 are the centers of the arrival time distributions for two peaks and fwhm_1 and fwhm_2 are their respective full widths at half maxima. Significant increases in R can be achieved by lengthening the device but are limited by the maximum voltage practical. To address this limitation, Clemmer and co-workers developed IM-MS instrumentation^{15–17} allowing as many as 100 passes of ions through a 1.8 m cyclic drift region and yielding a resolving power (RP) of ~1000 for triply protonated substance P.¹⁷ However, the sensitivity (although improved by multiple injections) was low, owing to ion losses in the drift regions and the repeated “chopping” of peak edges. More recently Giles and co-workers reported a cyclical (~1 m path) stacked ring ion guide using traveling waves (TW),¹⁸ and showed the resolution increased as a function of the number of cycles obtaining a collision cross section (CCS)-determined RP of ~240 for 12 passes of the singly protonated reversed sequence peptides GRGDS and SDGRG.¹⁹ Recently, structures for lossless ion manipulations (SLIM) have been introduced, which use arrays of electrodes patterned on two planar surfaces to create radio frequency (rf) and direct current (DC) ion confining fields. SLIM have been used for IM separations in a weak uniform field without loss of sensitivity.^{20–22} Additionally, SLIM components have been demonstrated for transmitting ions through turns,²² switching ions between two paths,²³ and ion storage over long times.²⁴ More recently we have developed TWIM-based SLIM^{25–27} utilizing relatively low traveling wave voltages (e.g., 40 V or less) to separate ions based upon their mobility-dependent ability to “keep up” with the traveling waves.^{28–30} The resolution of a TWIM separation is dependent on diffusion, similar to uniform drift fields, but is also dependent on the speed (s) of the TW. Importantly, the SLIM TWIM approach enabled the introduction of long serpentine path lengths, increasing the achievable IM resolution while avoiding the high voltages necessary for long path static drift fields.^{26,31} We have recently demonstrated a 13.5 m path length design providing resolution over five times greater than achieved using one meter drift tubes.^{26,31}

In the present work we report the initial implementation and application of a SLIM serpentine ultra-long path with extended routing (SUPER) high resolution TWIM module in conjunction with MS. This SLIM SUPER IM-MS utilizes a similar serpentine long path drift length and adds an ion switch at the end of the path to route ions either to the mass spectrometer or back to the beginning of the serpentine path. Therefore, the SLIM SUPER IM-MS platform reported here provides for much longer IM drift paths while maintaining essentially lossless ion transmission.

EXPERIMENTAL SECTION

The schematic diagram of the present multipass SLIM SUPER IM-MS system is displayed in Figure 1A. Ions were generated by a nanoelectrospray ionization source (3000 V) using a chemically etched emitter (20- μm i.d.) connected to a 30 μm i.d. fused-silica capillary (Polymicro Technologies, Phoenix, AZ) through a zero volume stainless steel union (Valco

Instrument Co. Inc., Houston, TX). Sample solutions were infused at 0.3 $\mu\text{L}/\text{min}$. Ions were introduced into the first stage of vacuum through a heated (130 °C) 500 μm i.d. stainless steel capillary (Figure 1A). After exiting the capillary, ions were accumulated in and released from an ion funnel trap (IFT, 950 kHz and ~ 200 V_{pp}) at 2.45 Torr.³² The inlet capillary was offset from the center axis of the IFT by 6 mm to minimize the transmission of higher mass particles through the IFT conductance-limiting orifice (2.50 mm i.d.), to the SLIM chamber maintained at 2.50 Torr (a 50 mTorr pressure differential, to further minimize any transfer of neutral particles from the source region into the SLIM chamber). The SLIM chamber was supplied with high-purity nitrogen filtered through hydrocarbon and moisture traps, and the pressure was measured using a convectron gauge (Granville-Phillips, Boulder, CO). The SLIM multipass TWIM module was designed based upon the 13.5 m long serpentine path SLIM we reported previously,^{26,31} and used the same rf, TW, and guard electrode arrangements and the same spacing between two surfaces (2.75 mm). The serpentine path utilized 6 rf strips (0.43 mm wide) and 5 TW electrode arrays (0.43 mm wide and 1.03 mm long); the gaps between electrodes were 0.13 mm. Guard electrodes (3.00 mm wide), fixed at 15 V DC for the entire study, were used to laterally confine ions along the ion path (Figure 1B). A power supply (GAA Custom Engineering, LLC, Kennewick, WA) provided an rf waveform of 822 kHz, 180° out-of-phase to adjacent rf electrodes to create pseudopotentials preventing ion loss to surfaces. The TW potential was applied to subsets of eight electrodes and repeated across the entire ion path, and involved the simultaneous application of a DC potential to 4 sequential electrodes in each subset, while the other four electrodes were maintained at ground potential.²⁵ The TW voltages applied are then stepped one electrode at a time to create the TW that propagates throughout the entire module. An ion switch was located at the end of the serpentine path and allowed ions to be routed to either the MS or another pass by applying a repulsive DC voltage to a set of electrodes in one of the two arrays (Figure 1C). Ions exit the multipass TW SLIM module into a 15 cm long “rear” ion funnel (820 kHz and ~ 120 V_{pp}) having a 5 V/cm DC gradient that was used to focus ions through a conductance limiting orifice (2.5 mm i.d.) to a differentially pumped region (0.34 Torr) containing a short rf-only quadrupole (1 MHz and ~ 130 V_{pp}). The TOF-MS was equipped with a 1.5 m flight tube (6224, Agilent Technologies, Santa Clara, CA). The signal from the TOF detector was routed into a U1084A 8-bit ADC digitizer (Keysight Technologies, Santa Rosa, CA) and processed using in-house control software written in C#. Agilent low concentration ESI tuning mix (Agilent, Santa Clara, CA) was directly infused for the evaluation of ion transmission and IM resolution. Equimolar (1 μM) oligosaccharide isomers lacto-*N*-hexaose (LNH, β -D-Gal-(1 \rightarrow 3)- β -D-GlcNAc-(1 \rightarrow 3)-[β -D-Gal-(1 \rightarrow 4)- β -D-GlcNAc-(1 \rightarrow 6)]- β -D-Gal-(1 \rightarrow 4)-D-Glc) and lacto-*N*-neohex-aose (LNnH, β -D-Gal-(1 \rightarrow 4)- β -D-GlcNAc-(1 \rightarrow 3)-[β -D-Gal-(1 \rightarrow 4)- β -D-GlcNAc-(1 \rightarrow 6)]- β -D-Gal-(1 \rightarrow 4)-D-Glc) (Sigma-Aldrich, St. Louis, MO) were prepared in 50% MeOH with 0.1% formic acid.

RESULTS AND DISCUSSION

Currently available IM-MS platforms often provide insufficient IM sensitivity and resolution for applications of interest. Higher resolution IM measurements in particular can potentially benefit a vast array of applications, contributing to their overall effectiveness in the

identification and quantification of mixture components. Of interest also is the ability to make such measurements with higher sensitivity and greater measurement throughput. SLIM TWIM provides a foundation for achieving far greater resolution than feasible with DTIM,^{22,25–27} facilitated by the use of multiple ion passes through a long serpentine path, and providing a basis for achieving theoretically unlimited IM resolution. We describe below our development and initial evaluation of such SLIM SUPER high resolution IM-MS instrumentation.

Lossless Ion Transmission over 1.1 Kilometers

For extended ion paths (with the length increasing with number of passes), ion transmission efficiency is critical for ion detection. In SLIM, an ion conduit is created by the rf time-varying potential from the parallel surfaces and guard bias static fields along ion tracks. Ions are moved using TW fields that have a predefined speed and amplitude. Previous studies with SLIM^{22,23,25–27} have shown the potential for lossless ion transmission using ion current measurements. In principle, ions could propagate in the direction of TW motion through a theoretically infinite long path.

To initially explore extended ion paths we used the Agilent tuning mix ions under moving condition (i.e., all ions are moving with TW traps at a specific speed, without ion activation and diffusion) where the arrival time is predictable (Figure 2A). We found the peak heights were unchanged for up to 81 passes (~1094 m). Consistently, the signal intensities (i.e., peak areas) show no significant decrease (i.e., ~10–15% variation) as a function of passes (Figure 2B). Thus, essentially lossless ion transmission is achievable over greatly extended path lengths in SLIM TWIM, potentially providing the basis for previously unobtainable levels of resolution.

Relationship between IM Separation Power, Resolution, and Multiple Passes

The resolving power of TWIM separations is dependent on diffusion in the same manner as in uniform drift fields, but is also dependent on the speed (s) of the TW. Ion mobilities allowing ions to move with the waves result in no separation (ions “surf” the wave), so resolving power (RP) is only meaningful when s is greater than the achieved ion velocity. The resolving power of DTIM (RP_{DT}) increases with square root of the path length, and experimental data has shown that RP_{DT} can extend to ~150 for conventional platforms.^{33–35} For DTIM, RP_{DT} is often experimentally determined using a single peak, an approach inappropriate for TW-based approaches. For instance, while no separation occurs under surfing conditions, the narrow peaks can correspond to very high RP. Since TWIM uses electric potential “waves” to propel ions through the ion path, rather than a static electric field, the RP achievable needs to be defined differently. Because of the complex nature of ion drift in TWs, a calibration curve is typically constructed to convert ion drift times to collision cross sections (Ω)^{36,37} and is related to TW drift time via an exponential function

$$\Omega = A \left[t_d^X \right] z \left[\frac{1}{\mu} \right]^{1/2} \quad (2)$$

where t_D is the TWIM drift time, z is the ion charge, μ is the reduced mass of the ion-neutral collision complex, A is a fitting parameter, and X is the exponential calibration factor. TWIM data and theory currently indicate that the accuracy of this conversion depends on the calibration data set and the instrumental conditions used for the calibration; the complete extent of potential Ω variations in TWIM measurements is presently unknown. The exponential relationship between Ω and t_D leads to different effective RP values in Ω space or t_D space. For instance, for a quadratic relationship between Ω and t_D , the TW collision cross section resolving power would be twice the temporal TW resolving power

($RP_{TW} = \frac{t}{\Delta t}$), where t is drift time and Δt is the peak fwhm.³⁸ Therefore, to prevent misrepresentation of resolving power by using a single peak definition with TWIM we introduce the term separation power (SP) to account for these factors. SP is defined as the average Ω resolving power for at least two baseline-resolved peaks

$$SP = \frac{\frac{\Omega_1}{\Delta\Omega_1} + \frac{\Omega_2}{\Delta\Omega_2} + \dots + \frac{\Omega_n}{\Delta\Omega_n}}{n} \quad (3)$$

where Ω is the known collision cross section for the peak and $\Delta\Omega$ is the peak width after conversion of the mobility spectrum from arrival time to collision cross section. Separation power therefore uses reference compounds with known collisional cross section, allowing straightforward comparisons between platforms. Additionally, we note that an estimate of SP can be provided for conventional IM separations after converting mobility spectra from drift time to Ω units.

In addition, we estimated the observed temporal IM resolution (R_{TW}) with multiple passes (Figure 3A) for Agilent tuning mix m/z 622 and 922 ions using $\frac{2(t_{922} - t_{622})}{\Delta t_{922} + \Delta t_{622}}$, where t_{922} and t_{622} represent the drift times, and Δt_{922} and Δt_{622} are the full width at half-maximum (fwhm) of the respective peaks. Figure 3B shows the SP of the present multipass SLIM SUPER IM module increased as anticipated with the length (or number of passes) for Agilent tuning mix m/z 622 and 922 ions. The IM spectra obtained at the same pass for m/z 622 and 922 ions are plotted with the number of passes ranging from 1 to 10 (because of the large mobility difference, the m/z 922 peaks will be lapped by the m/z 622 peak after the first pass). The results (Figure 3B) show that R_{TW} increases approximately with the square root of number of passes (i.e., length L), consistent with the observations of Giles and co-workers for up to 6 passes through a 1 m path.³⁹ In this work we find that after 40 passes through a 13.5 m path (i.e., 540 m), the R_{TW} increases to ~ 337 , more than 30-fold higher than reported using conventional DTIM or TWIM platforms (~ 10).^{18,30,40} In this initial work, the resolutions and separation powers for other compounds did not necessarily scale precisely with the square root of path length at higher pass numbers, and the origins of such observations are still subject to investigation. After conversion from drift time to CCS units, the SP was ~ 1860 after 40 passes (Figure 4). We note that the converted CCS resolution $R_{TW}^{\Omega} = 2 \frac{\Omega_{922} - \Omega_{622}}{\Delta\Omega_{922} + \Delta\Omega_{622}} = 339$ is similar to R_{TW}^t (337) calculated using drift times. Importantly, we note that much greater separation power and resolution should be obtainable with sufficiently large numbers of passes.

SLIM SUPER High-Resolution IM Separations Revealing New Oligosaccharide Features

Glycans are a major class of macromolecules and play an important role in cellular signaling, biomolecular interactions, protein structure and function.⁴¹ They are composed of different monosaccharides arranged in elaborate structures, and even subtle differences can modulate protein function. Considerable efforts have been made in developing techniques to routinely characterize individual structures in complex glycan mixtures with the majority being based on HPLC and LC-MS methodologies.⁴² However, intrinsic limitations to these approaches include their modest resolution and often low throughput nature, as well as the fact that tandem MS of their isomers often yield essentially identical fragmentation patterns in both positive and negative modes.⁴³

Thus, the present SLIM SUPER high resolution IM-MS platform represents a completely new tool for glyco-conjugate analysis. As an initial application in this work, we focused on the two human milk oligosaccharide (HMO) isomers lacto-*N*-hexaose (LNH) and lacto-*N*-neo-hexaose (LNnH). Both structures incorporate the same six monosaccharides and differ only in the regiochemistry in the lower antenna region, with the last galactose (Gal) residue linked to the penultimate *N*-acetylglucosamine (GlcNAc) via a β 1,3 glycosidic bond in LNH and a β 1,4 glycosidic bond in LNnH, as shown in Figure 5 left panel. Such a minor structural difference makes separation of these isomers difficult using conventional IM platforms. The multipass SLIM SUPER IM-MS can effectively differentiate these subtly different compounds.

We analyzed an equimolar mixture of LNH and LNnH oligosaccharides after 1 and 9 passes (Figures 5A and B), corresponding to 13.5 and 121.5 m, respectively. After 1 pass, the doubly charged $[M + K + H]^{2+}$ species (m/z 556) of LNH (0.140 s) and LNnH (0.133 s) are virtually baseline resolved. The peak width (fwhm) of LNnH (2.08 ms) is 0.76 ms wider than that of LNH, indicating potentially additional unresolved structural features. Indeed, with 3-fold higher IM resolution achievable after 9 passes, a new feature of LNnH was observed, which was not previously distinguished using conventional IM instruments.⁴³

CONCLUSIONS

In this work, we have developed and implemented a multipass SLIM SUPER high resolution IM-MS platform and initially demonstrated lossless ion transmission over 1.1 km, with the separation power proportional to the square root of passes (i.e., pass length), consistent with the theoretical predictions.³⁸ A 30-fold increase in IM resolution after 40 passes was demonstrated for Agilent tuning mix m/z 622 and 922 ions compared to conventional DTIM platforms. The separation power for m/z 622 and 922 ions was estimated to be \sim 1860, after 40 passes. In an initial application, two oligosaccharide isomers LNH and LNnH were baseline resolved after 1 pass, and a new conformational feature for LNnH was clearly distinguished for the first time after 9 passes.

This work highlights the potential of SLIM SUPER IM-MS for fast analyses of biological samples and other complex mixtures due to its combined ultrahigh sensitivity and ultrahigh IM resolution, and we believe the platform will have broad applicability. We have also recently demonstrated separations of lipid isomers⁴⁴ as well as differentiating isomers of cis/

trans plant natural products with clinical relevance.⁴⁵ Additionally, this technique will uniquely benefit targeted measurements, with the ability to switch unwanted species out of the drift path as well as select ions in regions for accumulation.²² Further increases of IM separation power and resolution should be achievable based upon additional passes or the implementation of longer path designs due to lossless ion transmission feasible in SLIM. We note that the recent development of a TWIM peak compression approach⁴⁶ based upon SLIM effectively mitigates the limitations because of diffusion (i.e., increased peak widths and decreased intensities) for greatly extended IM separations. The resolution achievable is ultimately limited by either the range of mobilities that can be covered without lapping, and where the overall length of the device determines the maximum resolution achievable over a given mobility range. The overlapping of lower mobility species by high mobility species at high pass numbers can likely be mitigated by the application of a peak compression approach⁴⁶ which we expect to enable complex mixture analysis without deleterious effects due to peak overlapping. This work suggests the possibility for SLIM SUPER IM-MS applications that have been previously intractable because of insufficient resolution, as well as new range of opportunities where the drift gas is modified to allow separations based upon ion-molecule interactions far too subtle for existing IM platforms.

Acknowledgments

Portions of this research were supported by grants from the National Institute of General Medical Sciences (P41 GM103493), the Laboratory Directed Research and Development Program at Pacific Northwest National Laboratory, and the U.S. Department of Energy Office of Biological and Environmental Research Genome Sciences Program under the Pan-omics Program. This work was performed in the W. R. Wiley Environmental Molecular Sciences Laboratory (EMSL), a DOE national scientific user facility at the Pacific Northwest National Laboratory (PNNL). PNNL is operated by Battelle for the DOE under contract DE-AC05-76RL0 1830.

References

1. Lanucara F, Holman SW, Gray CJ, Evers CE. *Nat Chem.* 2014; 6(4):281–294. [PubMed: 24651194]
2. Clemmer DE, Hudgins RR, Jarrold MF. *J Am Chem Soc.* 1995; 117(40):10141–10142.
3. Dear GJ, Munoz-Muriedas J, Beaumont C, Roberts A, Kirk J, Williams JP, Campuzano I. *Rapid Commun Mass Spectrom.* 2010; 24(21):3157–3162. [PubMed: 20941763]
4. Wyttenbach T, Pierson NA, Clemmer DE, Bowers MT. *Annu Rev Phys Chem.* 2014; 65:175–196. [PubMed: 24328447]
5. May JC, Goodwin CR, Lareau NM, Leaptrot KL, Morris CB, Kurulugama RT, Mordehai A, Klein C, Barry W, Darland E, Overney G, Imatani K, Stafford GC, Fjeldsted JC, McLean JA. *Anal Chem.* 2014; 86(4):2107–2116. [PubMed: 24446877]
6. Hsieh EJ, Bereman MS, Durand S, Valaskovic GA, MacCoss MJ. *J Am Soc Mass Spectrom.* 2013; 24(1):148–153. [PubMed: 23197307]
7. Shvartsburg AA, Li FM, Tang KQ, Smith RD. *Anal Chem.* 2006; 78(11):3706–3714. [PubMed: 16737227]
8. Shvartsburg AA, Danielson WF, Smith RD. *Anal Chem.* 2010; 82(6):2456–2462. [PubMed: 20151640]
9. Shvartsburg AA, Prior DC, Tang KQ, Smith RD. *Anal Chem.* 2010; 82(18):7649–7655. [PubMed: 20666414]
10. Shvartsburg AA, Smith RD. *Anal Chem.* 2011; 83(1):23–29. [PubMed: 21117630]
11. Prasad S, Belford MW, Dunyach JJ, Purves RW. *J Am Soc Mass Spectrom.* 2014; 25(12):2143–2153. [PubMed: 25267086]
12. Guevremont R. *J Chromatogr A.* 2004; 1058(1–2):3–19. [PubMed: 15595648]
13. Mason EA, Schamp HW. *Ann Phys.* 1958; 4(3):233–270.

14. Revercomb HE, Mason EA. *Anal Chem.* 1975; 47(7):970–983.
15. Merenbloom SI, Glaskin RS, Henson ZB, Clemmer DE. *Anal Chem.* 2009; 81(4):1482–1487. [PubMed: 19143495]
16. Glaskin RS, Valentine SJ, Clemmer DE. *Anal Chem.* 2010; 82(19):8266–8271. [PubMed: 20809629]
17. Glaskin RS, Ewing MA, Clemmer DE. *Anal Chem.* 2013; 85(15):7003–7008. [PubMed: 23855480]
18. Giles K, Pringle SD, Worthington KR, Little D, Wildgoose JL, Bateman RH. *Rapid Commun Mass Spectrom.* 2004; 18(20):2401–2414. [PubMed: 15386629]
19. Giles, K., Wildgoose, J.L., Pringle, S., Langridge, D., Nixon, P., Garside, J., Carney, P. Characterizing a T-Wave Enabled Multi-Pass Cyclic Ion Mobility Separator. *Proceedings of the American Society for Mass Spectrometry and Allied Topics*; St. Louis, MO, St. Louis, MO. May 31–June 4 2015; Santa Fe, NM: American Society for Mass Spectrometry; 2015.
20. Garimella SVB, Ibrahim YM, Webb IK, Tolmachev AV, Zhang XY, Prost SA, Anderson GA, Smith RD. *J Am Soc Mass Spectrom.* 2014; 25(11):1890–1896. [PubMed: 25257188]
21. Tolmachev AV, Webb IK, Ibrahim YM, Garimella SVB, Zhang XY, Anderson GA, Smith RD. *Anal Chem.* 2014; 86(18):9162–9168. [PubMed: 25152178]
22. Webb IK, Garimella SVB, Tolmachev AV, Chen TC, Zhang XY, Norheim RV, Prost SA, LaMarche B, Anderson GA, Ibrahim YM, Smith RD. *Anal Chem.* 2014; 86(18):9169–9176. [PubMed: 25152066]
23. Webb IK, Garimella SVB, Tolmachev AV, Chen TC, Zhang XY, Cox JT, Norheim RV, Prost SA, LaMarche B, Anderson GA, Ibrahim YM, Smith RD. *Anal Chem.* 2014; 86(19):9632–9637. [PubMed: 25222548]
24. Zhang XY, Garimella SVB, Prost SA, Webb IK, Chen TC, Tang KQ, Tolmachev AV, Norheim RV, Baker ES, Anderson GA, Ibrahim YM, Smith RD. *Anal Chem.* 2015; 87(12):6010–6016. [PubMed: 25971536]
25. Hamid AM, Ibrahim YM, Garimella SVB, Webb IK, Deng LL, Chen TC, Anderson GA, Prost SA, Norheim RV, Tolmachev AV, Smith RD. *Anal Chem.* 2015; 87(22):11301–11308. [PubMed: 26510005]
26. Deng LL, Ibrahim YM, Hamid AM, Garimella SVB, Webb IK, Zheng XY, Prost SA, Sandoval JA, Norheim RV, Anderson GA, Tolmachev AV, Baker ES, Smith RD. *Anal Chem.* 2016; 88(18):8957–8964. [PubMed: 27531027]
27. Hamid AM, Garimella SVB, Ibrahim YM, Deng LL, Zheng XY, Webb IK, Anderson GA, Prost SA, Norheim RV, Tolmachev AV, Baker ES, Smith RD. *Anal Chem.* 2016; 88(18):8949–8956. [PubMed: 27479234]
28. Thalassinos K, Slade SE, Jennings KR, Scrivens JH, Giles K, Wildgoose J, Hoyes J, Bateman RH, Bowers MT. *Int J Mass Spectrom.* 2004; 236(1–3):55–63.
29. Pringle SD, Giles K, Wildgoose JL, Williams JP, Slade SE, Thalassinos K, Bateman RH, Bowers MT, Scrivens JH. *Int J Mass Spectrom.* 2007; 261(1):1–12.
30. Giles K, Williams JP, Campuzano I. *Rapid Commun Mass Spectrom.* 2011; 25(11):1559–1566. [PubMed: 21594930]
31. Deng L, Ibrahim YM, Baker ES, Aly NA, Hamid AM, Zhang X, Zheng X, Garimella SVB, Webb IK, Prost SA, Sandoval JA, Norheim RV, Anderson GA, Tolmachev AV, Smith RD. *Chemistry Select.* 2016; 1(10):2396. [PubMed: 28936476]
32. Ibrahim Y, Belov ME, Tolmachev AV, Prior DC, Smith RD. *Anal Chem.* 2007; 79(20):7845–7852. [PubMed: 17850113]
33. Dugourd P, Hudgins RR, Clemmer DE, Jarrold MF. *Rev Sci Instrum.* 1997; 68(2):1122–1129.
34. Wu C, Siems WF, Asbury GR, Hill HH. *Anal Chem.* 1998; 70(23):4929–4938. [PubMed: 21644676]
35. Tang K, Shvartsburg AA, Lee HN, Prior DC, Buschbach MA, Li FM, Tolmachev AV, Anderson GA, Smith RD. *Anal Chem.* 2005; 77(10):3330–3339. [PubMed: 15889926]
36. Zhong YY, Hyung SJ, Ruotolo BT. *Analyst.* 2011; 136(17):3534–3541. [PubMed: 21445388]

37. Ruotolo BT, Benesch JLP, Sandercock AM, Hyung SJ, Robinson CV. *Nat Protoc.* 2008; 3(7):1139–1152. [PubMed: 18600219]
38. Shvartsburg AA, Smith RD. *Anal Chem.* 2008; 80(24):9689–9699. [PubMed: 18986171]
39. Giles, K., Wildgoose, J., Pringle, SD., Garside, J., Carney, P., Nixon, P., Langridge, DJ. Design and Utility of a Multi-pass Cyclic Ion Mobility Separator. Proceedings of the American Society for Mass Spectrometry and Allied Topics; Baltimore, Maryland, USA. June 14–15, 2014; Santa Fe, NM: American Society for Mass Spectrometry; 2014.
40. May JC, Goodwin CR, Lareau NM, Leaptrot KL, Morris CB, Kurulugama RT, Mordehai A, Klein C, Barry W, Darland E, Overney G, Imatani K, Stafford GC, Fjeldsted JC, McLean JA. *Anal Chem.* 2014; 86(4):2107–16. [PubMed: 24446877]
41. Dwek RA. *Chem Rev.* 1996; 96(2):683–720. [PubMed: 11848770]
42. Marino K, Lane JA, Abrahams JL, Struwe WB, Harvey DJ, Marotta M, Hickey RM, Rudd PM. *Glycobiology.* 2011; 21(10):1317–1330. [PubMed: 21566017]
43. Struwe WB, Baldauf C, Hofmann J, Rudd PM, Pagel K. *Chem Commun.* 2016; 52(83):12353–12356.
44. Wojcik R, Webb IK, Deng L, Garimella SV, Prost SA, Ibrahim YM, Baker ES, Smith RD. *Int J Mol Sci.* 2017; 18(1):183.
45. Zheng X, Renslow R, Makola M, Webb IK, Deng L, Thomas D, Govind N, Ibrahim Y, Kabanda M, Dubery I, Heyman H, Smith RD, Madala N, Baker E. *J Phys Chem Lett.* 2017; 8:1381–1388. [PubMed: 28267339]
46. Garimella SVB, Hamid AM, Deng L, Ibrahim YM, Webb IK, Baker ES, Prost SA, Norheim RV, Anderson GA, Smith RD. *Anal Chem.* 2016; 88:11877–11885. [PubMed: 27934097]

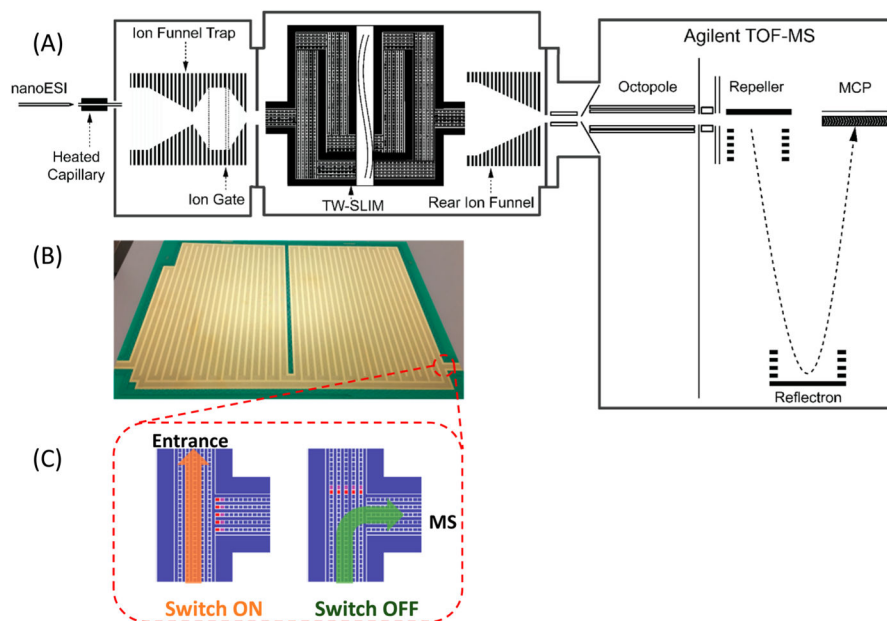


Figure 1. (A) Schematic diagram of the multipass SLIM SUPER IM-MS instrument used in this work; (B) photo of one of the two SLIM module surfaces; and (C) illustration of an ion switch (switch on, ion cycling; switch off, transmit ion to MS).

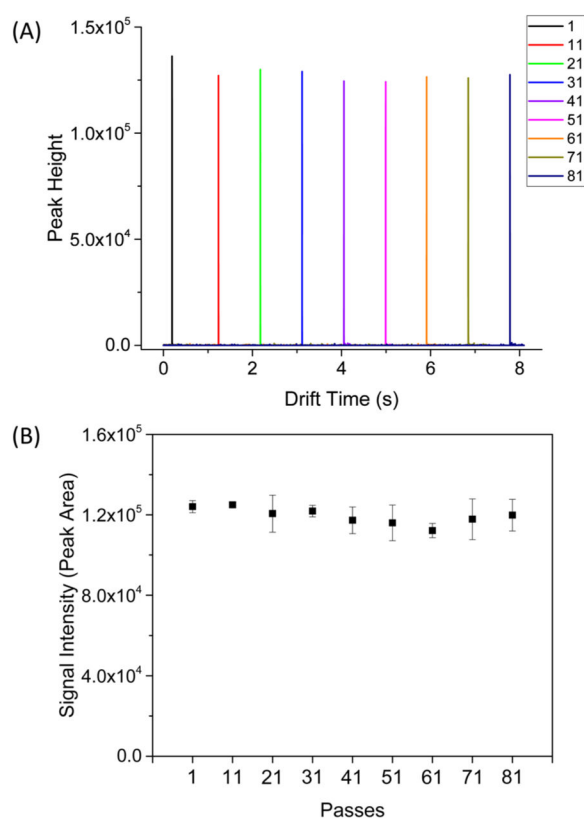


Figure 2.

(A) SUPER IM combined signal for ESI of Agilent tuning mix ions obtained at different passes (1–81) under the following surfing conditions: TW speed was 103 m/s, TW amplitude was 50 V, TW sequence was 11110000, guard =15 V, rf amplitude of 340 V_{pp} at 822 kHz, interboard gap was 2.75 mm, 2.50 Torr pressure. (B) The signal intensity (i.e., peak area) calculated plotted against the number of passes from replicate measurements.

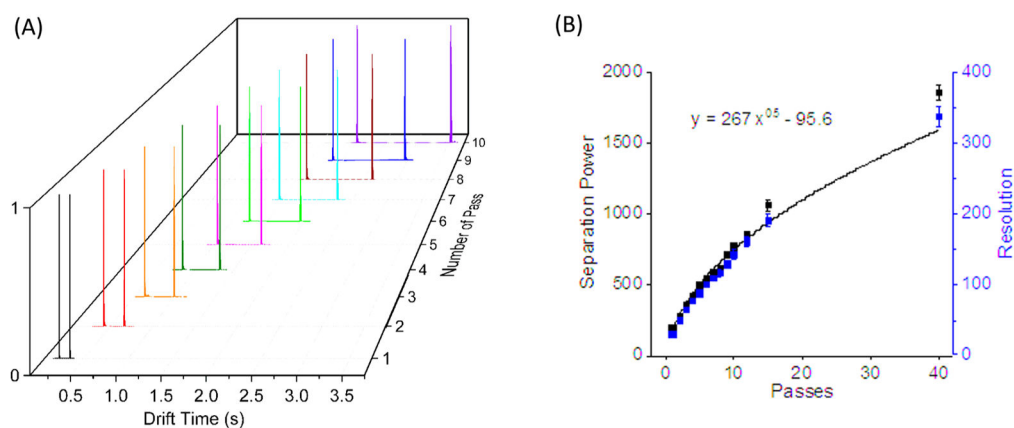


Figure 3.

(A) SUPER IM-MS separations for Agilent tuning mix m/z 622 and 922 ions acquired with 1–10 passes under conditions: TW speed was 206 m/s, TW amplitude was 30 V, TW sequence was 11110000, guard = 15 V, rf amplitude of 340 V_{pp} at 822 kHz, interboard gap was 2.75 mm, 2.50 Torr pressure. The calculated IM (B) separation power and resolution based upon the above IM spectra with 1–40 passes showing the observed IM separation power and resolution were both proportional to the square root of number of passes (i.e., path length).

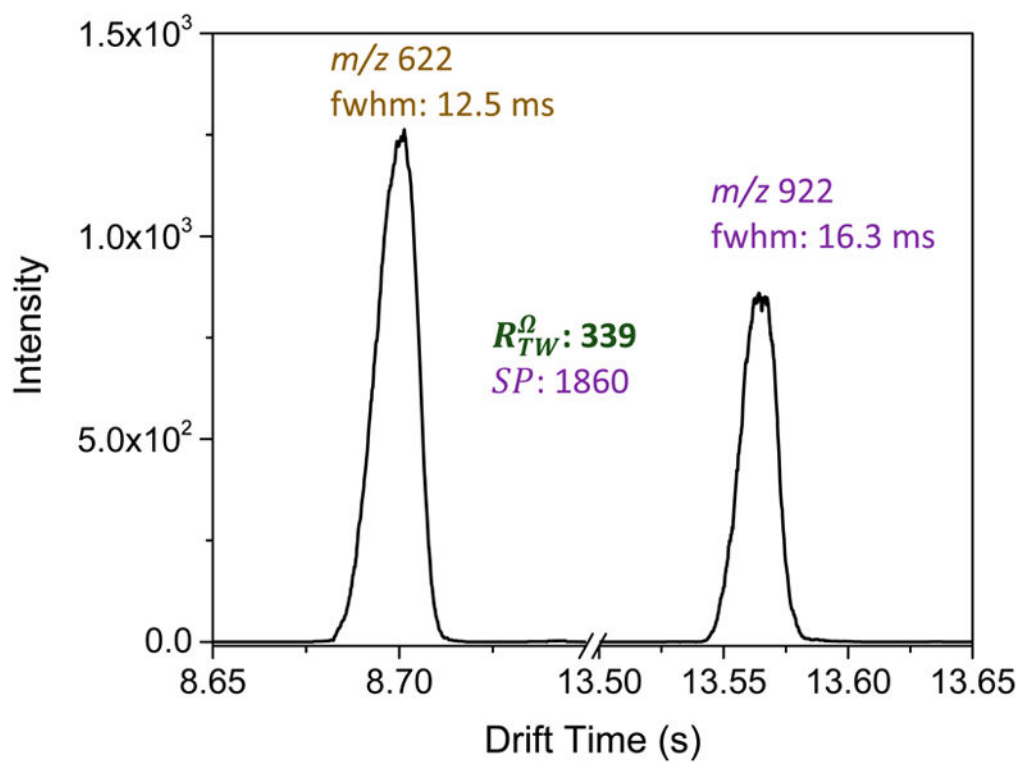


Figure 4. Merged SUPER IM spectrum of Agilent tuning mix m/z 622 and 922 ions obtained after 40 passes (~ 540 m) under the same conditions as Figure 3. The fwhm in drift time space, the separation power for m/z 622 and 922 ions and resolution between two ions were labeled as well.

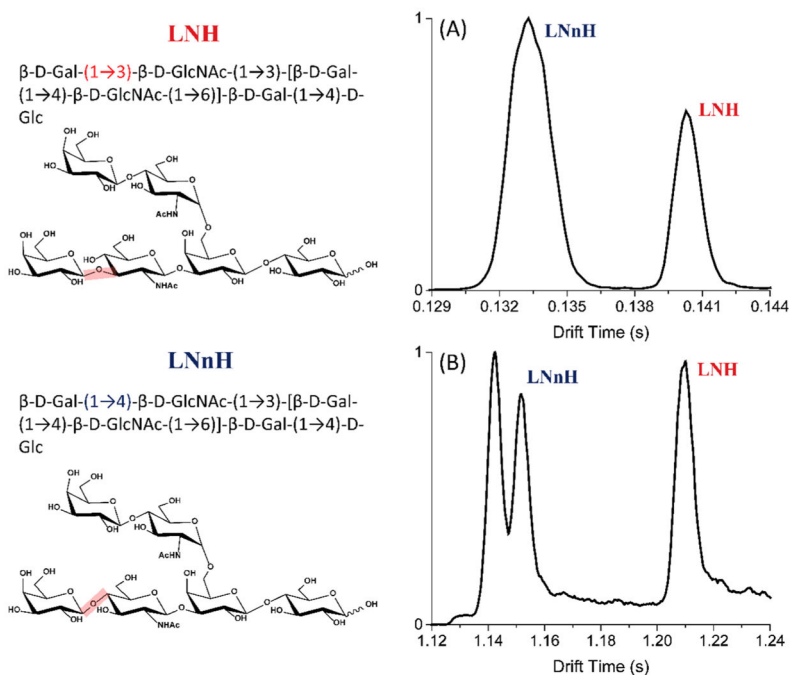


Figure 5. SLIM SUPER IM-MS separation of 1 μ M sugar isomers lacto-*N*-hexaose and lacto-*N*-neohexaose were obtained at (A) 1 pass and (B) 9 passes under the optimum conditions: TW speed of 206 m/s, TW amplitude of 30 V, guard bias of 15 V, RF amplitude of 340 V_{pp} at 822 kHz, and 2.75 mm gap at 2.50 Torr. The structures are illustrated in left panel.